
Fixation and Polarization in a Three-Species Opinion Dynamics Model

MAURO MOBILIA

Department of Applied Mathematics, School of Mathematics, University of Leeds, Leeds LS2 9JT, United Kingdom

PACS 02.50.-r – Probability theory, stochastic processes, and statistics
 PACS 89.75.Fb – Structures and organization in complex systems
 PACS 87.23.Kg – Dynamics of evolution

Abstract – Motivated by the dynamics of cultural change and diversity, we generalize the three-species constrained voter model on a complete graph introduced in [J. Phys. A **37**, 8479 (2004)]. In this opinion dynamics model, a population of size N is composed of “leftists” and “rightists” that interact with “centrists”: a leftist and centrist can both become leftists with rate $(1+q)/2$ or centrists with rate $(1-q)/2$ (and similarly for rightists and centrists), where q denotes the bias towards extremism ($q > 0$) or centrism ($q < 0$). This system admits three absorbing fixed points and a “polarization” line along which a frozen mixture of leftists and rightists coexist. In the realm of Fokker-Planck equation, and using a mapping onto a population genetics model, we compute the fixation probability of ending in every absorbing state and the mean times for these events. We therefore show, especially in the limit of weak bias and large population size when $|q| \sim N^{-1}$ and $N \gg 1$, how fluctuations alter the mean field predictions: polarization is likely when $q > 0$, but there is always a finite probability to reach a consensus; the opposite happens when $q < 0$. Our findings are corroborated by stochastic simulations.

Introduction. – Understanding how diversity is maintained and how traits copied by imitation spread are central issues in genetics, ecology, and in behavioral science [1–7]. In this context, there has recently been an upsurge of interest in statistical physics models predicting biological and cultural change, see e.g. [7,8], with relevant phenomena described by closely related models [9].

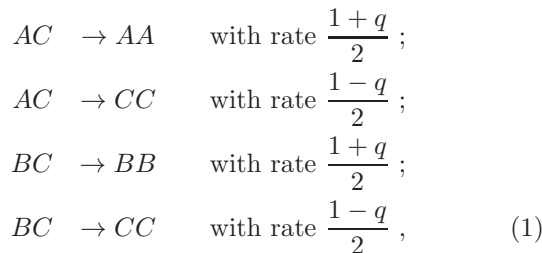
One of the basic issues in opinion dynamics is to understand the conditions under which consensus or diversity is reached from an initial population of individuals (agents) with different opinions. The voter model [10] is arguably the simplest and most popular opinion dynamics model [7]. In the voter model and in its variants [8], the evolution is implemented by allowing each agent, viewed as a “spin” [10], to adopt a new state in response to opinions in a local neighborhood. While the classic 2-state voter model unavoidably evolves towards consensus, it has recently been proposed that the competing features of *consensus* and *incompatibility* could be two realistic ingredients to help explain cultural diversity as an alternative to consensus [5,6]. The basic idea is that agents with sufficiently disparate opinions do not interact breaking up into distinct cultural states and in this case no consensus can

be reached (“incompatibility”), while individuals sharing close opinions may evolve towards a global consensus. Influential examples of models characterized by consensus and incompatibility are the Axelrod [5] and the bounded compromise models [6] that describe the formation and evolution of cultural domains. Recently, a (symmetric) discrete three-state version of the bounded compromise model was studied in low dimensions (where it exhibits slow non-universal kinetics) [11] and solved analytically in its zero-dimensional formulation [12]. In such a three-state opinion formation model, there are two species, A and B , respectively called “leftists” and “rightists”, that do not interact among them (incompatibility) [11,12]. However, A and B individuals interact with the third species, C (“centrists”), and thus indirectly compete to impose a consensus. Due to the A and B incompatibility, the final state can be either consensus or *polarization* with a frozen composition of leftists and rightists.

It is natural to generalize the three-state constrained voter model of Refs. [11,12] by assuming that the interaction between “extremists” (A and B individuals) and centrists is characterized by a bias q : extremists are more persuasive when $q > 0$, while centrists prevail when $q < 0$.

Here, our goal is to study how fluctuations alter the predictions of the mean field rate equations concerning the system's fate in the presence of a small bias q . We thus determine the “fixation probability” [13] of each absorbing state of the system (comprising N individuals on a complete graph) and compute the average times for these events to occur (mean fixation times). In fact, while polarization is generally the most probable outcome when $q > 0$ and centrism is likely to prevail when $q < 0$, we carefully analyze the effects of the bias on the system's fate, especially when the population size $N \gg 1$ is large and the bias $|q| \ll 1$ is weak but $Nq = \mathcal{O}(1)$, and determine the finite probability that the final state is a consensus when $q > 0$ and the frozen stationary state when $q < 0$.

The 3-state constrained voter model. – We consider a population of N individuals on a complete graph, N_A are of species A , N_B of type B and N_C of species C , with $N = N_A + N_B + N_C$. The idealized complete graph is used because of its simplicity and analytical tractability. In the language of the voter model, the species A and B represent “radical opinions” (e.g. leftists and rightists) while the type C stands for an “intermediate state” (e.g. centrists). Therefore, A and B individuals interact with C but do not interact among them. Hence, species A and B both strive to spread at the expense of C . This system therefore evolves through the interactions that species C has with types A and B . The latter follow the general prescriptions of the voter model and proceed by imitation: one individual is picked randomly and adopts the opinion of one of its random neighbor provided that at least one of the individual is of species C . In this way, the system's dynamics at each time increment can be schematically described by the following reactions:



where $-1 \leq q \leq 1$. The special case $q = 0$ was thoroughly studied in Ref. [12] and will therefore not be discussed here. The parameter q measures the bias towards polarization (when $q > 0$) or centrism (when $q < 0$). In the former situation extremists (A 's and B 's) are more persuasive than centrists (C 's), while in the latter centrism is the dominating and more persuasive opinion. As a consequence, we anticipate that polarization is the most probable final state when $q > 0$, while centrism consensus is expected to be the most likely stationary state when $q < 0$.

At mean field level, assuming a population of infinite size ($N \rightarrow \infty$) and the absence of any random fluctuations, the system dynamics is described by the following rate equations (REs) for the densities $a \equiv N_A/N$ and $b \equiv$

N_B/N of species A and B , respectively:

$$\frac{d}{dt}a = qa(1-a-b), \quad \frac{d}{dt}b = qb(1-a-b), \tag{2}$$

where we have used the fact that $a(t) + b(t) + c(t) = 1$. The REs (2) admit 3 absorbing fixed points, $(a, b, c) \equiv (a(\infty), b(\infty), c(\infty)) \in \{\mathcal{A} = (1, 0, 0), \mathcal{B} = (0, 1, 0), \mathcal{C} = (0, 0, 1)\}$ and a *line of fixed points* given by $\mathcal{AB} = (a, 1-a, 0)$, with $0 < a < 1$. In fact, the system (2) can be solved exactly, yielding [12]

$$a(t) = \frac{xe^{qt}}{1-(x+y)(1-e^{qt})}, \quad b(t) = \frac{ye^{qt}}{1-(x+y)(1-e^{qt})},$$

where x, y respectively are the initial densities of species A and B , i.e. $x = a(0)$ and $y = b(0)$. These results reveal that the line of fixed points is the stable solution when $q > 0$, i.e. in this case $(a, b, c) = (x/(x+y), y/(x+y), 0)$, with $a + b = 1$. On the other hand, when $q < 0$ and the bias favors the species C , one finds $a = b = 0$ and $c = 1$. Furthermore, we notice that the REs (2) predict that the ratio of the densities is conserved, i.e. $a(t)/b(t) = x/y$.

When the population size N is finite, demographic fluctuations can drastically alter the mean field predictions. In such a setting, the dynamics is no longer deterministic and the system's fate depends non-trivially on the bias strength and on the population initial composition, parametrized by the initial densities (x, y) . Within a stochastic formulation of the model, the moves (1) define a birth-death process [14], where, according to (1), the number of individuals of each species increases or decreases by one unit in each time step. A quantity that is central for our discussion is $P^{\mathcal{AB}}(x, y)$, the polarization fixation probability along the absorbing line \mathcal{AB} starting from an initial population composition $(x, y, 1-x-y)$. Hence, $P^{\mathcal{AB}}$ gives the probability to find the system locked into a *polarized* state where “extremists” (A 's and B 's) coexist without interacting. This probability obeys the following backward master equation [14]:

$$\begin{aligned}
&(T_x^+ + T_x^- + T_y^+ + T_y^-)P^{\mathcal{AB}}(x, y) = T_x^- P^{\mathcal{AB}}(x - \delta, y) \\
&+ T_x^+ P^{\mathcal{AB}}(x + \delta, y) + T_y^- P^{\mathcal{AB}}(x, y - \delta) + T_y^+ P^{\mathcal{AB}}(x, y + \delta),
\end{aligned} \tag{3}$$

where, in the limit $N \gg 1$, the transition rates are $T_x^\pm \equiv (1 \pm q)x(1-x-y)/2$ and $T_y^\pm \equiv (1 \pm q)y(1-x-y)/2$, with $\delta = N^{-1}$. This *two-dimensional* equation has to be supplemented by the boundary conditions: $P^{\mathcal{AB}}(x, 0) = P^{\mathcal{AB}}(0, y) = 0$ and $P^{\mathcal{AB}}(x, 1-x) = 1$. By Taylor-expanding (3) to second-order in δ , one finds

$$\left\{ s[x\partial_x + y\partial_y] + \frac{1}{2}[x\partial_x^2 + y\partial_y^2] \right\} P^{\mathcal{AB}}(x, y) = 0, \tag{4}$$

where we have introduced the parameter $s \equiv Nq$. When $|s| \gg 1$, the diffusion term on the left-hand-side of (4) is negligible in front of the deterministic drift term, while the

opposite occurs when $|s| \ll 1$. This implies that the interesting situation arises when s is of order one, i.e. when $N \gg 1$ and $|q| \sim N^{-1}$; otherwise one would essentially recover the mean field predictions of (2) when $|s| \gg 1$, or the results of Ref. [12] when $|s| \ll 1$. It is also useful to notice that the associated backward Fokker-Planck (FP) differential operator \mathcal{L}_{bFP} reads [14]:

$$\mathcal{L}_{\text{bFP}} = \frac{(1-x-y)}{2N} [2s(x\partial_x + y\partial_y) + x\partial_x^2 + y\partial_y^2] \quad (5)$$

A *one-dimensional* version of \mathcal{L}_{bFP} often appears in population genetics [1] and evolutionary game theory [4].

Fixation Probabilities. – We have seen that the mean field treatment (2) predicts that the line \mathcal{AB} and the fixed point \mathcal{C} are the system's attractor when $q > 0$ and $q < 0$, respectively. The quantity P^{AB} , that obeys (4), and the probability density $F_a^{AB}(x, y)$ that the system's final state has coordinate $(a, 1-a)$ along the absorbing line, are central to study the system's fate in the presence of fluctuations. These quantities are related by $P^{AB}(x, y) = \int_0^1 da F_a^{AB}(x, y)$. Hence, $F_a^{AB}(x, y)$ obeys the same backward FP equation (4) as P^{AB} but with the boundary conditions $F_a^{AB}(0, y) = F_a^{AB}(x, 0) = 0$ and $F_a^{AB}(x, 1-x) = \delta(a-x)$. As in Ref. [12], Eq. (4) turns out to be *separable* and *exactly solvable*. To obtain its solution, it is useful to introduce the polar coordinates (ρ, θ) such that $\sqrt{x} = \rho \cos \theta$ and $\sqrt{y} = \rho \sin \theta$. In these coordinates, with $0 \leq \rho \leq 1$ and $0 \leq \theta \leq \pi/4$, Eq. (4) becomes:

$$\begin{aligned} & [(4s\rho - \rho^{-1})\partial_\rho + \partial_\rho^2] P^{AB}(\rho, \theta) \\ & + \rho^{-2} (\{\tan \theta - \cot \theta\} \partial_\theta + \partial_\theta^2) P^{AB}(\rho, \theta) = 0. \end{aligned} \quad (6)$$

with boundary conditions $P^{AB}(\rho = 0, \theta) = 0$ and $P^{AB}(\rho = 1, \theta) = 1$. The probability density F_a^{AB} also obeys the equation (6) but with the boundary conditions $F_a^{AB}(\rho = 0, \theta) = 0$ and $F_a^{AB}(\rho = 1, \theta) = \delta(a - \cos^2 \theta)$. Following Ref. [12], we write P^{AB} and F_a^{AB} in the form $\sum_n c_n R_n(\rho) u_n(\theta) \sin(2\theta)$, where the $R_n(\rho)$ and $u_n(\theta)$ are the eigenvectors (with eigenvalues λ_n) of the following radial and angular Sturm-Liouville problems, respectively:

$$\begin{aligned} \rho^2 \frac{d^2 R_n}{d\rho^2} + \rho \frac{dR_n}{d\rho} [4s\rho^2 - 1] - \lambda_n R_n &= 0 \\ \frac{d^2 u_n}{d\theta^2} - \frac{3}{4} \left(\frac{1}{\sin^2 \theta} + \frac{1}{\cos^2 \theta} \right) u_n + (1 + \lambda_n) u_n &= 0 \end{aligned} \quad (7)$$

The solution to the radial equation (7) with boundary condition $R_n(0) = 0$ reads $R_n(\rho) \propto e^{-s\rho^2} \rho^{-2n-1} I_{n+1/2}(s\rho^2)$, where I_n is the modified Bessel function of first kind and order n [15]. The equation (7) for the angular function $u(\theta)$ coincides with a stationary Schrödinger equation in a Pöschl-Teller potential whose solution is $u_n(\theta) \propto \sqrt{\sin(2\theta)} P_{n+1}^1(\cos(2\theta))$, where P_n^1 denotes an associate Legendre polynomial of first order [12, 16]. The eigenvalues are found to be $\lambda_n = 4(n+1)(n+2)$ and the coefficients c_n are determined using the orthogonality of the P_n^1 's together with

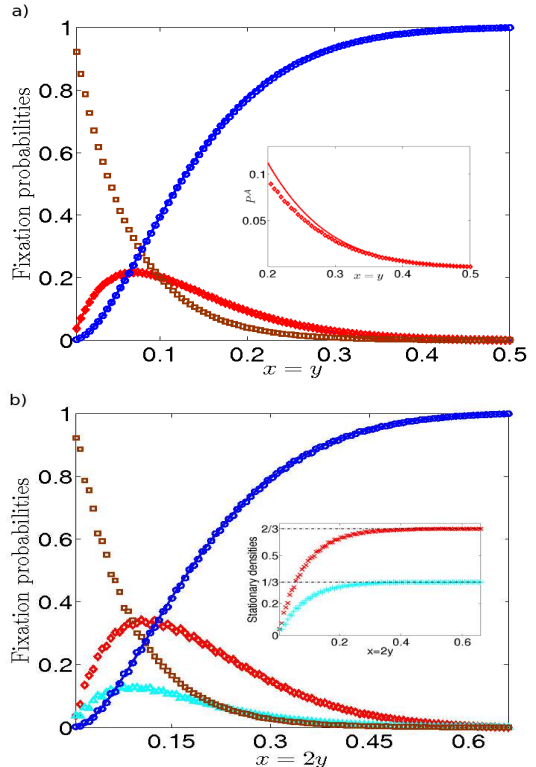


Fig. 1: (*Color online*). Fixation probabilities for $s > 0$ as functions of x : P^A (\diamond), P^B (\triangle), P^C (\square); P^{AB} (\circ) is compared with (9) (solid curve). Parameters are $N = 200$, $s = 4$ (i.e. $q = 0.02$). (a) Initial density of A is $x = y$ and $P^A = P^B$. Inset: Comparison of P^A with its analytical approximation, see text. (b) Initial density of A is $x = 2y$. Inset: final densities of species A (\times) and B ($+$) as functions of $x = 2y$. Numerical results have been averaged over 2×10^5 samples.

the boundary conditions for F_a^{AB} and P^{AB} [12]. This leads to

$$\begin{aligned} F_a^{AB}(x, y) &= \sqrt{\frac{xy}{x+y}} e^{s(1-x-y)} \sum_{n=1}^{\infty} \left(\frac{2n+1}{n(n+1)} \right) \\ &\times \left\{ \frac{I_{n+1/2}(s(x+y))}{I_{n+1/2}(s)} \right\} P_n^1 \left(\frac{x-y}{x+y} \right) \frac{P_n^1(2a-1)}{\sqrt{a(1-a)}}. \end{aligned} \quad (8)$$

Since $P^{AB}(x, y) = \int_0^1 da F_a^{AB}(x, y)$, using the properties of the associate Legendre polynomials [15], one also obtains

$$\begin{aligned} P^{AB}(x, y) &= 2 \sqrt{\frac{xy}{x+y}} e^{s(1-x-y)} \sum_{n \text{ odd}}^{\infty} \left(\frac{2n+1}{n(n+1)} \right) \\ &\times \left\{ \frac{I_{n+1/2}(s(x+y))}{I_{n+1/2}(s)} \right\} P_n^1 \left(\frac{x-y}{x+y} \right), \end{aligned} \quad (9)$$

where the subscript “ n odd” means that the sum runs over odd integers n . Since P^{AB} is the polarization fixation probability, the probability that the system's final state is consensus (with either A , B , or C) is $1 - P^{AB}$.

The quantities P^{AB} and the fixation probabilities of the absorbing states \mathcal{A} , \mathcal{B} and \mathcal{C} , respectively denoted P^A , P^B

and P^C , are related by $P^A(x, y) + P^B(x, y) + P^{AB}(x, y) = a + b = 1 - P^C(x, y)$. In fact, as C 's interact identically with A 's and B 's, a mapping onto a population genetics model where extremists are regarded as mutants of a single class yields $P^C = \frac{e^{-2s(x+y)} - e^{-2s}}{1 - e^{-2s}}$ (see below). Furthermore, the fixation probabilities and the species density are related by $a = P^A(x, y) + \int_0^1 da' a' F_{a'}(x, y)$ and $b = P^B(x, y) + P^{AB}(x, y) - \int_0^1 da' a' F_{a'}(x, y)$, with $P^B(x, y) = P^A(y, x)$.

When $|s| \ll 1$, $I_{n+1/2}(s(x+y))/I_{n+1/2}(s) \approx (x+y)^{n+1/2}$ [15] and, with (8) and (9), one obtains $\frac{F_{a;q \neq 0}^{AB}(x, y)}{F_{a;q=0}^{AB}(x, y)} = \frac{P_{q \neq 0}^{AB}(x, y)}{P_{q=0}^{AB}(x, y)} = [1 - s\{x+y-1\} + \mathcal{O}(s^2)]$. From this expression and the compact result $P_{q=0}^{AB}(x, x) = 1 - \frac{1-4x^2}{\sqrt{1+4x^2}}$ obtained in [12], we infer $P^{AB}(x, x) \approx 6(1+s)x^2$ when $x = y \ll 1$. Hence, at low initial density $x = y$ and for weak bias ($|s| \ll 1$), P^{AB} is a quadratic polynomial in x with an amplitude proportional to s .

Fixation probabilities when $s > 0$. When $s > 0$, we find that the fixation probability $P^{AB}(x, y)$ displays a sigmoid shape, that steepens when s increases, interpolating monotonically between 0 (when $x+y \ll 1$) and 1 (for $x+y \rightarrow 1$), see Fig. 1. The agreement between the analytical prediction (9) and the results of stochastic simulations (obtained using the Gillespie algorithm [17]) is excellent, as illustrated in Fig. 1. This figure also shows that P^C steeply decays to zero when $x+y$ increases, as expected from its analytical expression. Furthermore, P^A and P^B display positive skewness and maxima around the initial densities (x_*, y_*) such that $P^{AB}(x_*, y_*) = P^C(x_*, y_*)$ ($x_* + y_* \approx 0.157$ in Fig. 1(a)). Moreover, as shown in the inset of Fig. 1(b), the stationary densities steadily approach their mean field values, i.e. $a \rightarrow x/(x+y)$ and $b \rightarrow x/(x+y)$, when $x+y \gtrsim 0.30$. In such a regime, one thus has $a \approx \frac{x}{x+y} = P^A(x, y) - \int_0^1 da' a' F_{a'}(x, y)$ and, with (8), this yields the following approximation for the fixation probability of A : $P^A(x, y) \approx \frac{x}{x+y} - \sqrt{\Delta} e^{s(1-x-y)} \sum_{n=1}^{\infty} \left(\frac{2n+1}{n(n+1)} \left\{ \frac{I_{n+1/2}(s(x+y))}{I_{n+1/2}(s)} \right\} \right) P_n^1(\Delta)$, where $\Delta \equiv (x-y)/(x+y)$. The inset of Fig. 1(a), shows that the agreement between this approximation and the results of numerical simulations increases with $x = y \gtrsim 0.20$. A similar approximation gives $P^B \approx 1 - P^{AB}(x, y) - P^A(x, y)$.

Fixation probabilities when $s < 0$. When $s < 0$, the bias is towards the absorbing state $C = (0, 0, 1)$ and the fixation probabilities P^A and P^B are vanishingly small. For small initial densities of A and B (i.e. $x+y \ll 1$), the probability of reaching the absorbing line AB is also very small ($\lesssim N^{-1}$). However, this fixation probability P^{AB} grows monotonically when $x+y$ increases and, according to (9) and as shown in Fig. 2(a,b), approaches the value one when $x+y \rightarrow 1$. Figure 2 shows that the system's most likely fate is either to end up in the state C or on the line AB . To determine a concise and accurate approximation of P^{AB} , one can use a mapping onto a population genetics

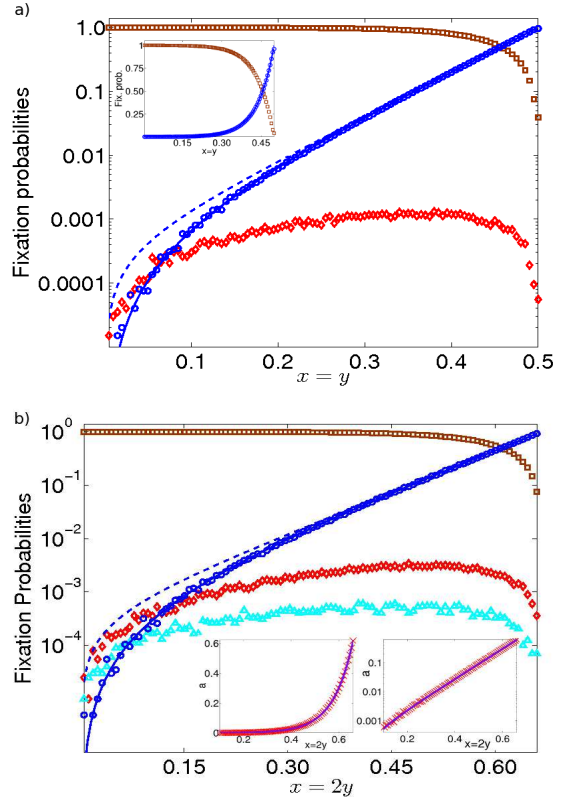


Fig. 2: (Color online). Same as in Fig. 1, with $s = -4$ in semi-log scale, and comparison with (9) (solid curve) and (10) (dashed curve), see text. The initial density of A is $x = y$ in (a) and $x = 2y$ in (b). Inset of (a): P^C and P^{AB} in linear scale. Insets of (b): stationary density of A (\times) as function of $x = 2y$ compared with the analytical expression (solid curves) given in the text, in linear (left) and semi-log (right) scales.

model where C is considered as a “wild-type” allele and both A and B species are regarded as forming a single-class deleterious allele [1]. In this situation, the probability $P^{AB}(x, y) = P^{AB}(x+y)$ corresponds to the fixation of the (single-class) “mutants” and depends only on $x+y$ and s . The angular dependence therefore drops out from (6) and, with the (new) boundary conditions $P^{AB}(x+y=0) = 0$ and $P^{AB}(x+y=1) = 1$, one obtains the following approximation for P^{AB} :

$$P^{AB}(x+y) \simeq \frac{e^{2|s|(x+y)} - 1}{e^{2|s|} - 1}. \quad (10)$$

As shown in Fig. 2, this result is found to be an excellent approximation of P^{AB} when $x+y \gtrsim 0.30$. In such a regime $P^A \approx P^B \approx 0$ and $P^{AB}(x+y) \simeq 1 - P^C(x+y)$ (see inset of Fig. 2(a)). Using (10), one can obtain the stationary densities $b \simeq a(y/x)$ and $a \simeq \left(\frac{x}{x+y}\right) \left(\frac{e^{2|s|(x+y)} - 1}{e^{2|s|} - 1}\right)$. The excellent agreement between this expression and numerical simulations is demonstrated in the insets of Fig. 2 (b).

Mean Fixation times. – The mean times necessary to reach the absorbing states, also called the mean fixation

times (MFTs), are quantities of great interest in evolutionary dynamics [1, 3, 4, 7, 8]. Here, the unconditional MFT to reach *any* of the system's absorbing states is a function $\tau(x, y)$ of the initial density (x, y) obeying the backward FP equation $\mathcal{L}_{\text{bFP}}(x, y)\tau(x, y) = -1$ [see (5)] with boundary conditions $\tau(1, 0) = \tau(0, 1) = \tau(0, 0) = \tau(a, 1 - a) = 0$ [1, 14]. Such an equation can be solved by using an exact mapping onto a suitable population genetics model. In fact, since we are interested in the *unconditional* MFT, and species C does not make any distinction between A and B individuals, as seen above, the latter can be considered as belonging to a single “mutant type” class that interacts with the “wild type” C [1]. In this formulation, the equation for τ becomes one-dimensional with two absorbing states: either only wild-type individuals (consensus with C) or only mutants (either A or B consensus, or polarization in a frozen mixture of A 's and B 's). The unconditional MFT thus depends only on the initial density $x + y$ of extremists (A 's and B 's): $\tau(x, y) = \tau(x + y)$. Hence, with the variable $w \equiv x + y$, one obtains:

$$\frac{w(1-w)}{N} \left[2s \frac{d\tau(w)}{dw} + \frac{d^2\tau(w)}{dw^2} \right] = -1, \quad (11)$$

with $\tau(0) = \tau(1) = 0$. Eq. (11) frequently appears in population genetics, where it describes the MFT in a diallelic haploid population in the presence of selection of (weak) intensity $|q| = |s|/N \ll 1$ [1] (see also [4]). An interesting property of (11) is its invariance under the transformation $(w, s) \rightarrow (1-w, -s)$. This implies that $\tau(w)$ for $s > 0$ coincides with $\tau(1-w)$ for $s < 0$, see Fig. 3. Equation (11) can be solved by standard means (see e.g. [4, 14] and references therein) yielding a cumbersome expression. The latter takes a more compact form for the special value $w = 1/2$, when it reads:

$$\begin{aligned} \tau &= \frac{N}{s(1+e^s)} [e^{2s}\text{Ei}(-2s) + (e^s - 1) \ln(2|s|)] \\ &+ \frac{N}{2se^s(1+e^s)} [e^s(e^s - 1)\gamma_E + \text{Ei}(s) - \text{Ei}(2s)] \\ &+ \frac{N}{2s(1+e^s)} [2\text{Ei}(s) - 2e^s(e^s + 1)\text{Ei}(-s)], \quad (12) \end{aligned}$$

where $\text{Ei}(x) \equiv \int_{-\infty}^x \frac{e^t}{t} dt$ denotes the exponential integral and $\gamma_E = 0.5772\dots$ is Euler-Mascheroni's constant [15]. From the general expression of $\tau(x + y)$, one finds that the unconditional MFT scales linearly with the system size N , i.e. $\tau(x + y) = Nf_\tau(s, x + y)$, where f_τ is a scaling function. Such a scaling relationship is fully confirmed by the numerical results reported in Fig. 3(a,b). We can infer from the latter that f_τ has an inverted u-shape dependence on $w = x + y$ and skewness towards small values of w for $s > 0$ and large values of w for $s < 0$, see Fig. 3(a,b). This is a consequence of the $(w, s) \rightarrow (1-w, -s)$ symmetry obeyed by $\tau(x + y)$. The *conditional* mean fixation times, τ^S , to reach the absorbing states $\mathcal{S} \in (\mathcal{A}, \mathcal{B}, \mathcal{C}, \mathcal{AB})$ can be obtained by solving

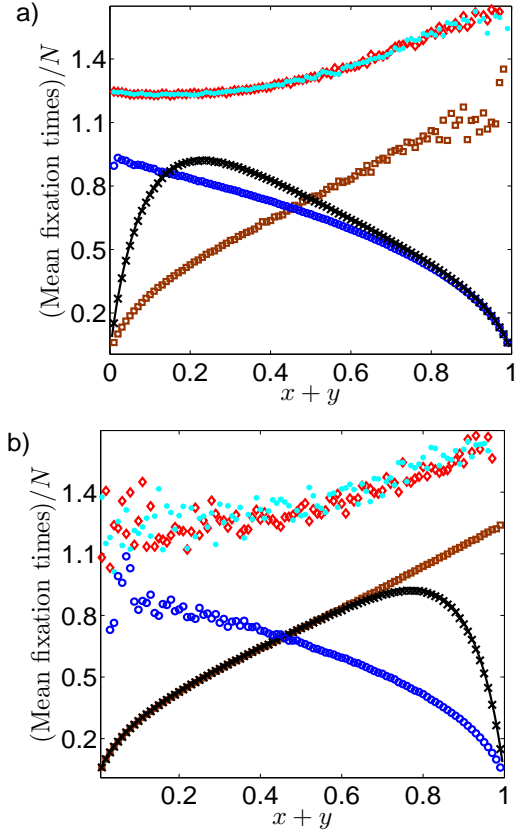


Fig. 3: (*Color online*). The normalized unconditional mean fixation time (MFT) τ/N (\times), compared with the solution of Eq. (11) (solid curve), and the (normalized) conditional MFTs τ^A/N (\diamond), τ^B/N (\bullet), τ^C/N (\square), τ^{AB}/N (\circ), see text. The parameters are $N = 200$, $x = y$ (initial A density), $s = 4$ in (a) and $s = -4$ in (b). The maxima of the unconditional MFTs are $\tau(0.22) \approx 0.94N$ in (a) and $\tau(0.78) \approx 0.94N$ in (b). The numerical results have been averaged over 2×10^5 samples.

$\mathcal{L}_{\text{bFP}}(x, y)[P^S(x, y)\tau^S(x, y)] = -P^S(x, y)$, where $P^S(x, y)$ is the fixation probability of the state \mathcal{S} , with the appropriate boundary conditions [1, 14]. Except for τ^C , these equations cannot be mapped onto one-dimensional problems and are difficult to solve. However, as $P^{AB} \rightarrow 1$ when $w \rightarrow 1$ and $s > 0$, we infer that in this regime the equation for τ^{AB} coincides with (11) and therefore $\tau^{AB} \simeq \tau$, as confirmed by Fig. 3(a). Similarly, since $P^C \rightarrow 1$ when $w \ll 1$ and $s < 0$, τ^C coincides with τ in such a regime, see Fig. 3(b). The numerical results reported in Fig. 3(a,b) show that all τ^S 's scale linearly in N (and monotonically with $x + y$), in a manner that appears to be independent of the sign of s . In fact, while the results for τ^A and τ^B in Fig. 3(b), where $s < 0$, and those of Fig. 3(a), where $s > 0$, are comparable, the former are more noisy than the latter. Furthermore, as also found for the special case $q = 0$ [12], the extremists MFTs, i.e. τ^A and τ^B , are always the longest mean fixation times.

Conclusion. – We have generalized a basic three-state opinion dynamics model introduced in Refs. [11, 12] and considered a finite population of N individuals consisting of leftists, rightists and centrists interacting on a complete graph. Motivated by recent studies concerning the formation of cultural diversity, the system’s dynamics is characterized by two competing features: (i) “extremists” (leftists A ’s or rightists B ’s) interact with centrists (C ’s) and at each elemental step an extremist can become a centrist with rate $(1 - q)/2$, while a centrist can become either leftist or rightist with rate $(1 + q)/2$; (ii) extremists do not interact. The former feature drives the system towards *consensus* while the latter accounts for *incompatibility* and leads to a frozen steady state of A ’s and B ’s (polarization). The parameter q denotes a bias favoring polarization when $q > 0$ and centrism when $q < 0$.

This three-species voter model is characterized by three absorbing fixed points (one for each species) and an absorbing line where a frozen mixture of extremists coexist (polarization). Here, we have studied the model’s final state properties and showed that fluctuations drastically alter the mean field predictions in the presence of a small bias. In fact, while polarization is generally the most probable outcome when $q > 0$ there still is a finite probability to attain a consensus, and the opposite situation arises when $q < 0$. Our results are particularly relevant in the limit of large population size $N \gg 1$ and vanishing bias $|q| \ll 1$ with $s \equiv Nq = \mathcal{O}(1)$ finite, where the fluctuations and the deterministic drift are of the same intensity. Such a situation corresponds to the “weak selection limit” frequently considered in life and behavioral sciences [1, 3, 4].

The polarization fixation probability, P^{AB} , has been obtained analytically by solving a (separable) backward Fokker-Planck equation and our results have been checked against stochastic simulations. Via a mapping onto a population genetics model, we have shown that when $s < 0$ P^{AB} approximately grows exponentially with the initial density $x + y$ of extremists, whereas the centrist fixation probability P^C decays (approximately) exponentially with $x + y$ when $s > 0$. The mean fixation times (MFTs) have been computed and found to scale linearly with N (see Fig. 3). Furthermore, the unconditional MFT τ has been shown to satisfy $\tau(x + y, s) = \tau(1 - x - y, -s)$.

Our results show that mean field rate equations cannot describe the final state of a simple opinion-dynamics model in the presence of a small bias. This further illustrates the pertinence of statistical physics methods to describe the evolutionary dynamics of models of cultural diversity.

Acknowledgments: Sid Redner is gratefully acknowledged for a useful discussion.

REFERENCES

- [1] J. F. Crow and M. Kimura, *An Introduction to Population Genetics Theory* (The Blackburn Press, New Jersey, 1970); W. J. Ewens, *mathematical Population Genetics* (Springer, U.S.A., 2004).
- [2] R. M. May, *Stability and Complexity in Model Ecosystems* (Princeton University Press, U.S.A., 1973); S. P. Hubbell, *The Unified Neutral Theory of Biodiversity and Biogeography* (Princeton University Press, U.S.A., 2001).
- [3] M. A. Nowak, *Evolutionary Dynamics* (Belknap Press, 2006); G. Szabó and G. Fáth, Phys. Rep. **446** 97 (2007).
- [4] A. Traulsen and C. Hauert, arXiv:0811.3538v1; J. Cremer, T. Reichenbach, and E. Frey, New J. Phys. **11** 093029 (2009); M. Mobilia and M. Assaf, EPL **91**, 10002 (2010); J. Stat. Mech., **P09009** (2010).
- [5] R. Axelrod, J. Conflict Resolution **41**, 203 (1997); R. Axelrod, *The complexity of cooperation*, (Princeton University Press, 1997); C. Castellano, M. Marsili, and A. Vespignani, Phys. Rev. Lett. **85**, 3536 (2000); K. Klemm *et al.*, Phys. Rev. E **67**, 045101 (2003).
- [6] G. Deffuant *et al.*, Adv. Complex Syst. **3**, 87 (2000); R. Hegselmann and U. Krause, Journal of Artificial Societies and Social Simulation **5**, issue 3 (2002); G. Weisbuch *et al.*, Complexity **7**, 55 (2002); E. Ben-Naim, P. L. Krapivsky, and S. Redner, Physica D **183**, 190 (2003); F. Slanina, Eur. Phys. J. B **79**, 99 (2011).
- [7] C. Castellano, S. Fortunato, and V. Loreto, Rev. Mod. Phys. **81**, 591 (2009).
- [8] S. Galam, J. Stat. Phys. **61**, 943 (1990); Physica A **274**, 132 (1999); Eur. Phys. J. B **25**, 403 (2002); K. Sznajd-Weron, J. Sznajd, Int. J. Mod. Phys. C **11**, 1157 (2000); M. Mobilia, Phys. Rev. Lett. **91**, 028701 (2003); M. Mobilia and S. Redner, Phys. Rev. E **68**, 046106 (2003); V. Sood and S. Redner, Phys. Rev. Lett. **94**, 178701 (2005); M. S. de la Lama *et al.*, Eur. Phys. J. B **51**, 435 (2006); T. Antal, V. Sood, and S. Redner, Phys. Rev. Lett. **96**, 188104 (2006); M. Mobilia, A. Petersen, and S. Redner, J. Stat. Mech., **P08029** (2007); V. Sood, T. Antal, and S. Redner, Phys. Rev. E **77**, 041121 (2008); R. Lambiotte and S. Redner, EPL **82**, 18007 (2008); I. J. Benczik *et al.*, EPL **82**, 48006 (2008); L. Dall’Asta and T. Galla, J. Phys. A: Math. Theor. **41** 435003 (2008); R. A. Blythe, J. Phys. A: Math. Theor. **43** 385003 (2010).
- [9] R. A. Blythe and A. J. McKane, J. Stat. Mech. **P07018** (2007); K. S. Korolev *et al.*, Rev. Mod. Phys. **82**, 1691 (2010).
- [10] T. M. Liggett, *Interacting Particle Systems* (Springer, U.S.A., 1985).
- [11] F. Vazquez, P. L. Krapivsky, and S. Redner, J. Phys. A: Math. Gen. **36**, L61 (2003).
- [12] F. Vazquez and S. Redner, J. Phys. A: Math. Gen. **37**, 8479 (2004).
- [13] The term “fixation probability of state S ” is adopted from population genetics [1] and refers to the probability that the system final state is the absorbing state S .
- [14] C. W. Gardiner, *Handbook of Stochastic Methods* (Springer, U.S.A., 2002); N. G. van Kampen, *Stochastic Processes in Physics and Chemistry*, (North-Holland, Amsterdam, 1992); S. Redner, *A Guide to First-Passage Processes* (Cambridge University Press, U.S.A., 2001).
- [15] M. Abramowitz and I. Stegun (editors), *Handbook of Mathematical Functions*, (Dover, New York, 1965).
- [16] S. Flügge, *Practical Quantum Mechanics* (Springer, Berlin, 1994).
- [17] D. T. Gillespie, J. Comput. Phys. **22**, 403 (1976).